Climate Simulation since Industrial Revolution

Contact person Akio Kitoh
Head, First Research Laboratory
Climate Research Department
Meteorological Research Institute
Nagamine 1-1, Tsukuba, Ibaraki, 305-0052 Japan
Tel: +81-29-853-8594 Fax: +81-29-855-2552
E-mail: kitoh@mri-jma.go.jp

Total Budget for FY2002-FY2004 79,197,000Yen (**FY2004**; 25,998,000Yen)

Key Words Greenhouse Gas, Solar Activity, Radiative Forcing, 20th Century Climate Simulation, Climate Model

1. Introduction

The observed climate record shows an increase of global mean surface air temperature of about 0.6°C in the last 100 years. There are many factors that force climate change such as greenhouse gases (CO_2, CH_4, N_2O and halocarbons), natural and anthropogenic aerosols, volcanic activity, and solar variability. If a climate model (global atmosphere-ocean coupled general circulation model; CGCM) that includes all the observed forcing is found able to reproduce historical observed climate change, then such a model can be used assess the impact of each forcing on climate change by a series of systematically designed numerical experiments.

In addition, the observations show decadal-scale variability in sea surface temperature (SST), surface air temperature and sea level pressure among others. It is not known whether this decadal variability is due to internal variability of the earth's climate system or a response of the climate system to any forcing agent. The modeling study can also be used to answer such a question by performing ensemble simulations with different initial conditions but with the same forcing by separating response to forcing from internal variability.

2. Research Objective

In this study, we perform historical climate simulation with the Meteorological Research Institute (MRI) climate model for the period ever since instrumental observed records are available. The model is forced by the observed data such as well-mixed greenhouse gases (CO_2, CH_4, N_2O and halocarbons), natural and anthropogenic sulfate aerosols in the troposphere, radiative forcing due to volcanic activity, and solar variability. Then we assess the impact of forcing factors on climate change.

3. Result

(1) Observed data and forcing data: collection and analysis

Solar irradiance data and volcanic aerosol data since the industrial revolution are collected and their quality is checked to produce external forcing data for the MRI climate model. In addition, long-term observed data of surface pressure and temperature are collected and analyzed with other available data focusing on the long-term variations

and/or atmospheric response to external forcing variations.

The relation between North Atlantic Oscillation (NAO) index and solar activity is investigated during winters for 100 years from 1900 to 1999. The circulation/temperature pattern is categorized according to the solar activity intensity. For weak solar activity years, NAO pattern localizes in the Atlantic and its significant temperature pattern appears only over Europe, while for strong solar activity years, negative-positive seesaw pressure pattern extends from the north Atlantic to Eurasia, and the action center in high latitudes covers the entire polar region. Corresponding surface temperature variations appear over two continents, the North America and Eurasia, indicating the close link between NAO and northern hemispheric scale temperature variation.

The effect of solar 11-year activity is also examined on the modulation of polar night jet oscillation (PJO), using 21 years reanalysis data from 1979 to 1999. The difference between solar max and solar minimum averages shows that positive and negative temperature anomalies, respectively, quasi-periodically propagate downward in polar region. Also zonal-mean zonal wind anomalies, initiated in the upper stratosphere, propagate quasi-periodically poleward and downward. In addition, EP-flux anomalies propagate toward weak zonal-mean zonal wind area. These features coincide with those of PJO, demonstrating that solar 11-year variations modulate PJO. As for southern hemisphere, similar modulation of PJO appears. The common feature in both winter hemispheres indicates that enhanced heating anomaly in the summer hemisphere due to solar max irradiance increase strengthens westerly jet from upper stratosphere to mesosphere through the increase in meridional temperature gradient and that this westerly-jet anomaly affects the triggering of PJO intensity and phase.

The effect of the 11-year solar cycle modulation on the Southern Annular Mode (SAM) in the Southern Hemisphere is examined through analysis of observational data from 1968 to 2001. It is found that the year-to-year variability of the October-November mean SAM differs significantly according to the solar activity. In high solar activity years, the SAM signal extends to the upper stratosphere during October to December and activity in the troposphere lasts until autumn, whereas in low solar activity years, the SAM signal is confined almost inside the troposphere from October to December and it disappears by January. This situation is very similar to that observed for the modulation of the winter mean North Atlantic Oscillation in the Northern Hemisphere.

(2) Atmospheric GCM simulation with historical SST/sea-ice data

We have evaluated the climate variations and changes over the 130-year period from 1872 to 2001 simulated by the Atmospheric General Circulation Model (AGCM) called "MJ98" (Shibata et al., 1999) [4)]. The model has the horizontal resolution of about 270 km. The model has 30 vertical levels with the top at 0.4 hPa corresponding to altitude of 55 km.

Six-member ensemble integrations were performed from 1872 to 2001, forcing with the observed Sea Surface Temperature (SST) and sea ice data "HadISST1" (Rayner et al., 2003) [3)]. As for greenhouse gases, the observed concentration of carbon dioxide CO_2 increasing from 288 ppmv in 1872 to 370 ppmv in 2001, was given homogeneously to the whole atmosphere without any seasonal cycle. The concentration of methane CH_4 was specified as 1650 ppbv, and nitrogen oxide N_2O as 306 ppbv. The concentration of both CH_4 and N_2O are kept constant in time and space in the whole atmosphere.

Figure 1 shows the time series of annual anomalies of global average land-surface air temperature for 130 years from 1872 to 2001. Observational data by Jones et al. (2001) [2)] is used. Model well reproduces observed positive trend for the whole 130-year period.

However, simulated temperatures are higher than observations before 1910 and lower than observations after 1980. This leads to the model's underestimation of observed positive trend for the whole period. Observation shows positive trend from 1910 to 1945, negative trend from 1946 to 1975, and large positive trend from 1976 to 2001. It is noteworthy that model well reproduces all these three observed trends, which means that model can also reproduce the decadal variability land-surface air temperature.

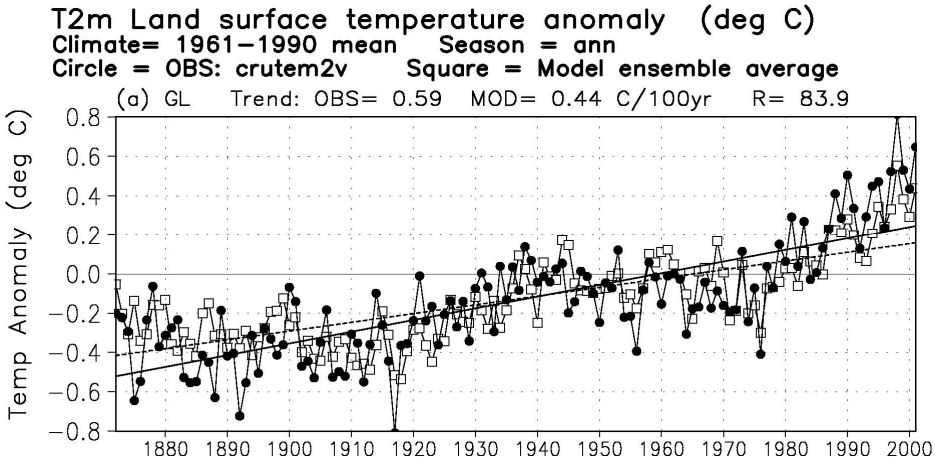

Figure 1 Annual anomalies of global average land-surface air temperature (°C), 1872 to 2001, relative to 1961 to 1990 mean values. Black circle ● indicates observation. The slant solid line is the linear regressed line by least square fitting to observed time series. White square □ indicates ensemble average of model simulations. The dashed line is the linear regressed line for model. Values of observed trend (OBS) and model trend (MOD) are shown at the top outside the panel in the unit °C/100yr.

Same calculations have applied to all four seasonal mean global average land-surface air temperatures (Fig. 2). The model well reproduces positive trend for all seasons, although their magnitude are underestimated. Seasonality of simulated trends was weaker than that of observed.

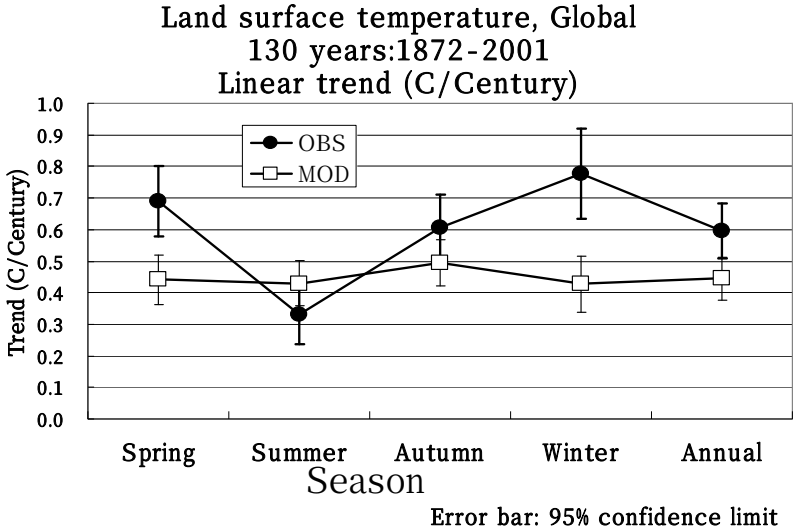

Figure 2 Dependence of observed and simulated trends (Deg C/ 100 yr) on seasons for global average land-surface air temperature. Black circle ● indicates observation. White square □ indicates ensemble average of model simulations. Error bars show the 95% confidence limits.

Precipitation extreme values in an AGCM ensemble were also investigated to clarify the model's reproducibility and the statistical characteristics of the extremes in the AGCM. Observational precipitation data by Hulme et al. (1998) [1)] is used with the period of 1901-1998. The extreme values are computed for each member, and for a set of the 6-member ensemble. The maximum extreme values of the 200-yr return period were almost equal between the members with no statistically significant differences except for the Sahara desert (Fig. 3). The mean of the maximum extreme values were also almost equal to the maximum extreme values obtained from the 6-member ensemble. Therefore, the maximum extreme values of precipitation are robustly estimated when a single integration is available. The maximum values estimated from the observation were not well reproduced, especially in the inland areas of the continents.

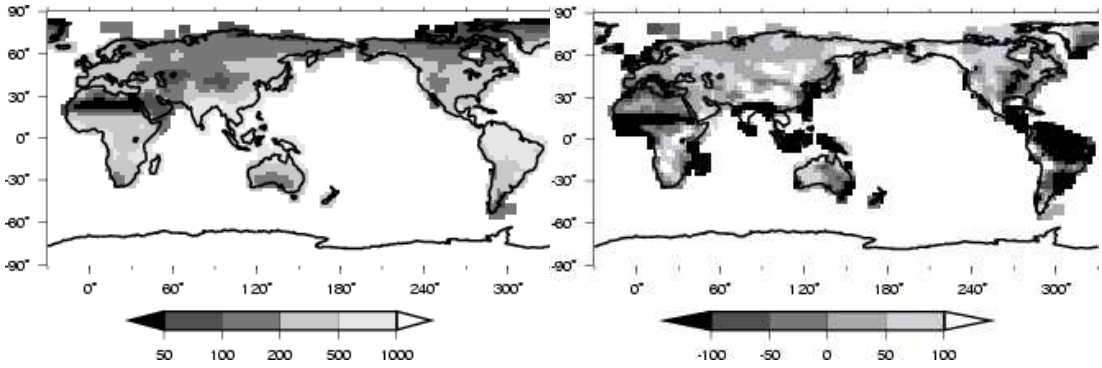

Figure 3 200-yr probability maximum monthly precipitation. Left: the ensemble mean of the 6-member simulations, and right: the observation.

(3) Study on the historical climate simulation with a climate model and the impact assessment of forcing factors on climate change

The historical climate simulation with the climate model is performed by forcing with well-mixed greenhouse gases (CO_2, CH_4, N_2O, and halocarbons), natural and anthropogenic sulfate aerosols in the troposphere, radiative forcing due to volcanic activity, and solar variability for the period since 1850, and the simulation results are analyzed. The model simulated interdecadal change of the global average surface air temperature agree with the observed ones since mid-nineteenth century.

With the ensemble simulation, the interdecadal variation is analyzed by defining the ensemble mean as response to the external forcing and the residual from it as the internal variability. We investigated the interdecadal variation of the Arctic Oscillation. In the surface pressure pattern, response to the external forcing exhibits annular pattern and the temporal variation of the principal component reveals overall increase in the twentieth century with enhanced increase trend after 1970s. These characteristics are consistent with observed interdecadal variation of the Arctic Oscillation.

Although the annular pattern in the surface pressure is bearing some similarity with the internal variability, it is characterized by more zonal symmetric and a relatively weaker anomalies in the midlatitude North Atlantic and North Pacific. As for the meridional-vertical structure of the atmosphere, the internal variability is characterized by a barotropic structure implying a similar dynamical mechanism for the AO that is dominated by interaction between waves and meridional circulation. On the other hand, the external forcing response exhibits opposite signs in temperature anomalies between the

troposphere and stratosphere, which can be explained by thermal responses to the radiative forcing due to increased greenhouse gases.

It is suggested that the zonal wind becomes stronger in the midlatitude stratosphere, by an integrated response to a stratospheric cooling due to GHG radiative forcing and a tropopause uplift due to surface warming. Changes in planetary wave activity associated with the intensified westerly in the stratosphere induce a tropospheric zonal wind dipole, which is coherent with surface AO pattern (probably through a meridional circulation change). Positive feedback from the ocean to the AO-like forcing is significant in seasons when the stormtrack is active (early winter and early spring) and in regions which are the action center of AO.

References

1) Hulme, M., T. J. Osborn and T.C. Johns, 1998: Precipitation sensitivity to global warming: Comparison of observations with HadCM2 simulations. *Geophys. Res. Letts.*, **25**, 3379-3382. http://www.cru.uea.ac.uk/~mikeh/datasets/global/
2) Jones, P. D., T. J. Osborn, K. R. Briffa, C. K. Folland, E. B. Horton, L. V. Alexander, D. E. Parker and N. A. Rayner, 2001: Adjusting for sampling density in grid box land and ocean surface temperature time series. *J. Geophys. Res.*, **106**, D4, 3371-3380. http://www.cru.uea.ac.uk/cru/data/temperature/
3) Rayner, N. A., D. E. Parker, E. B. Horton, C. K. Folland, L. V. Alexander, D. P. Rowell, E. C. Kent, and A. Kaplan, 2003: Global analyses of sea surface temperature, sea ice, and night marine air temperature since the late nineteenth century. *J. Geophys. Res.*,**108**(D14),4407,doi:10.1029/2002JD002670. http://dss.ucar.edu/datasets/ds277.3/
4) Shibata, K., H. Yoshimura, M. Ohizumi, M. Hosaka, and M. Sugi, 1999: A simulation of troposhpere, stratosphere and mesosphere with an MRI/JMA98 GCM. *Papers in Meteorl. and Geophys.*, **50**, 15-53.